Scaling in the quantum Hall regime of graphene Corbino devices

Eva C. Peters, A. J. M. Giesbers, Marko Burghard, and Klaus Kern

Citation: Appl. Phys. Lett. **104**, 203109 (2014); doi: 10.1063/1.4878396
View online: http://dx.doi.org/10.1063/1.4878396
View Table of Contents: http://aip.scitation.org/toc/apl/104/20
Published by the American Institute of Physics

Scaling in the quantum Hall regime of graphene Corbino devices

Eva C. Peters,[1] A. J. M. Giesbers,[1,2] Marko Burghard,[1] and Klaus Kern[1,3]
[1]*Max-Planck Institute for Solid State Research, Heisenbergstrasse 1, D-70569 Stuttgart, Germany*
[2]*Molecular Materials and Nanosystems, Eindhoven University of Technology, NL-5600 MB Eindhoven, The Netherlands*
[3]*Institut de Physique de la Matière Condensée, Ecole Polytechnique Fédérale de Lausanne, CH-1015 Lausanne, Switzerland*

(Received 18 February 2014; accepted 5 May 2014; published online 22 May 2014)

The scaling behavior of graphene devices in Corbino geometry was investigated through temperature dependent conductivity measurements under magnetic field. Evaluation of the Landau level width as a function of temperature yielded a relatively low temperature exponent of $\kappa = 0.16 \pm 0.05$. Furthermore, an unusually large value close to 7.6 ± 0.9 was found for the universal scaling constant γ, while the determined inelastic scattering exponent of $p = 2$ is consistent with established scattering mechanisms in graphene. The deviation of the scaling parameters from values characteristic of conventional two-dimensional electron gases is attributed to an inhomogeneous charge carrier distribution in the Corbino devices. Direct evidence for the presence of the latter could be gained by spatially resolved photocurrent microscopy away from the charge neutrality point of the devices. © *2014 AIP Publishing LLC*.
[http://dx.doi.org/10.1063/1.4878396]

Scaling theory deals with carrier localization in an electron system, and thus can provide relevant information about the properties of the carriers in the quantum Hall regime. In the edge state picture, the integer quantum Hall effect (QHE) in two-dimensional electron gases (2DEGs) arises from localized states in the tails of individual Landau levels, which lead to quantized plateaus in the Hall resistance. By comparison, the states in the center of the Landau levels (LLs) are extended, and the delocalization of their wave functions is governed by a localization length, which follows a power law behavior away from the LL centers.[1] This decay is associated with a universal critical scaling exponent.[2,3] In recent years, the scaling behavior of graphene has attracted increasing interest.[4–6] Thus far, this property has been experimentally addressed by measurements using graphene Hall bar devices. In exfoliated graphene, $\kappa = 0.41$ has been determined for the derivatives ($d\rho_{xy}/dB$) at the critical point from the plateau $\nu = 0$ to plateau $\nu = 1$ transition,[4] while $\kappa = 0.37$ has been documented for the half width in ρ_{xx} of the first LL.[4] Furthermore, the scaling of the $\nu = 0$ to $\nu = 1$ inter-plateau transition in epitaxial graphene has been reported to belong to the same universality class as the same transition in mechanically exfoliated graphene.[7] In this Letter, we use graphene Corbino devices to explore the scaling properties of exfoliated graphene. The Corbino device geometry offers a two-fold advantage. First, the longitudinal conductivity can be directly compared to theory, without the need of a tensor inversion like in case of Hall bar measurements. Second, it provides a high resolution at very low longitudinal conductivities.

Fig. 1(a) depicts one Corbino disk device used to directly measure the longitudinal conductivity in the quantum Hall effect regime of graphene. In the first device fabrication step, graphene was deposited by mechanical exfoliation onto a degenerately doped Si substrate (serving as back gate) covered with 300 nm of thermally grown silicon oxide. Cylindrical Ti/Au contacts were then defined on monolayer graphene flakes by standard e-beam lithography and subsequent metal evaporation. While the outer ring had an inner radius of 3.5 μm and width of 2 μm, the inner ring had an inner radius of 1 μm and width of 1 μm. This resulted in a Corbino device comprising an inner radius of $r_1 = 1.5\,\mu$m and an outer radius of $r_2 = 2.5\,\mu$m, enclosing a graphene ring with a width of $L_{sample} = 1.0\,\mu$m. In addition to these Corbino devices denoted by "size 1.0," also smaller Corbino devices scaled down by a factor of 0.75 were investigated (denoted by "size 0.75"). The devices were further processed by reactive ion etching of the graphene outside the Corbino disk area, in order to disconnect it from the surrounding graphene/graphite and the central contact. Finally, the center contact was connected to the center contact lead via a gold air-bridge contact, as shown in the bottom of Fig. 1(a). Optionally, the finished devices were thermally annealed in argon at 120 °C for several hours in order to enhance the sample quality.

The magnetic field and temperature dependent electrical conductivity of the Corbino devices were measured by standard two-terminal lock-in technique, using sufficiently low currents to avoid heating effects. The longitudinal conductivity σ_{xx} was calculated from the measured conductance $G = I/V$ with the aid of the geometry factor A_0 according to

$$\sigma_{xx} = GA_0 = \frac{G}{2\pi}\ln\left(\frac{r_1}{r_2}\right). \quad (1)$$

In Fig. 1(b), the two-point resistance and conductivity of a typical Corbino device of size 1.0 is displayed as a function of filling factor ν at 12 T and 1.4 K. The filling factor is related to the applied back gate voltage V by

$$\nu = \frac{nh}{eB} = \frac{\alpha V h}{eB}, \quad (2)$$

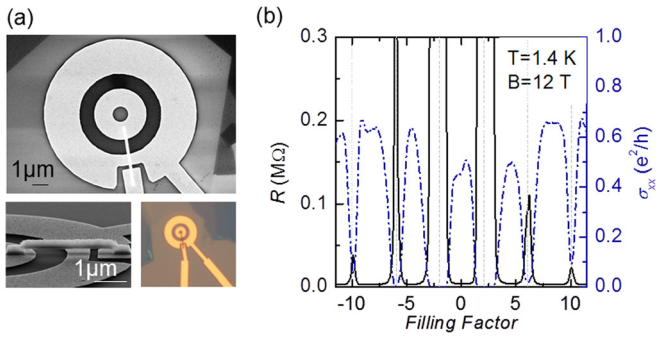

FIG. 1. (a) Scanning electron micrograph in top view (top image) and side view (bottom left image) of a size 1.0 graphene Corbino device. The image on the bottom right is an optical micrograph of the device (top view). (b) Two-point resistance and longitudinal conductivity of the Corbino device at 1.4 K and 12 T.

where n is the charge carrier concentration, h Planck's constant, e is the electron charge, B is the applied magnetic field, and α is the gate coupling constant. In the plot, minima in σ_{xx} and maxima in $R_{2-point}$ can be clearly discerned at filling factors $\nu = \pm 2, \pm 6, \pm 10, \ldots$ corresponding to the complementary quantum Hall plateaus. For all size 1.0 devices, the onset of additional minima in σ_{xx} could be observed at low temperatures, indicative of LL splitting due to degeneracy lifting.[8–10] Such splitting emerged up to higher LLs, which reflects a good sample quality, in accordance with the charge neutrality point (CNP) occurring close to zero back gate voltage (V_{CNP} between −2.0 V and 8.5 V) for all measured samples. Thermal annealing further amplified the splitting as a consequence of the enhanced carrier mobility. That degeneracy lifting is detectable even though the LL width $\Delta\nu$ is larger for the Corbino devices in comparison to Hall bar devices testifies that the Corbino geometry is particularly suited to resolve interaction effects. In Hall bar devices subjected to a similar processing as the present Corbino devices, the LL width is of the order of 0.8 at T = 1.5 K.[4] In general, the LL width may be overestimated in case of degeneracy lifting, as a non-completely resolved splitting makes the feature, which is actually composed of two separate levels, appear broader. However, this effect can be eliminated by evaluating the temperature dependent width, since the splitting only depends on magnetic field, but not on temperature.

For the smaller Corbino devices, as exemplified in Fig. 2(a), degeneracy lifting could not be observed even if the CNP was shifted close to zero back gate voltage through annealing. This absence could be due to scattering between the edge channels, akin to the shortening of the high and low potential lines around hotspots in graphene Hall-bar devices with a size of approximately 500 nm,[11,12] which is close to the 0.75 size Corbino devices. Fig. 2(a) furthermore illustrates the influence of temperature on the longitudinal conductivity, which manifests itself by a width $\Delta\nu$ of the peaks with increasing temperature. This width provides useful information about the scattering mechanisms that are operative in graphene,[13–15] although contact resistance effects may have to be taken into account.[16] For conventional 2DEGs, the LL width scales with temperature according to $\Delta\nu \propto T^{\kappa}$, where the T exponent $\kappa \approx 0.42$.[1–3] The same dependency has been reported for graphene Hall bar devices,[4] except for high

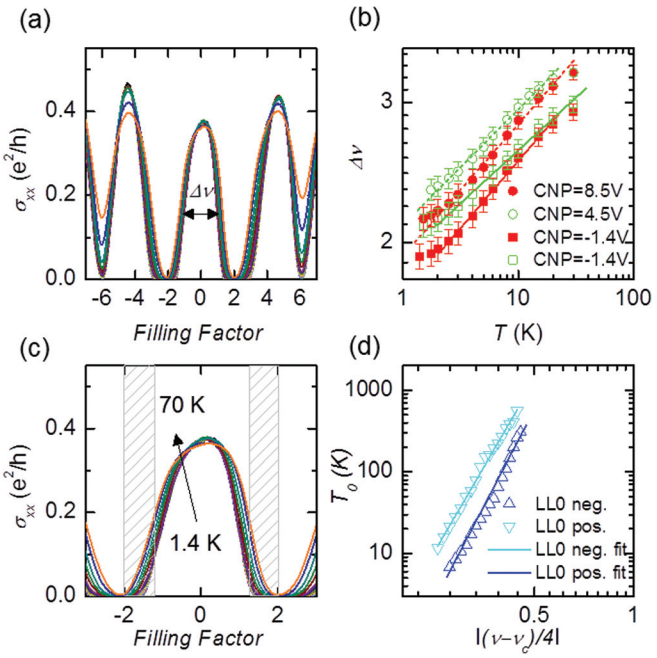

FIG. 2. (a) Longitudinal conductance of a size 1.0 Corbino device in the quantum Hall regime at temperatures between 1.4 and 70 K. (b) Landau level full width at half maximum as a function of temperature for two different 1.0 devices (filled red vs. open green symbols) on the same substrate prior (circles) and after annealing at 120 °C (squares). (c) Temperature dependence of the tails of the lowest LL. (d) Characteristic temperature T_0 obtained by analysis of the zeroth LL tails in the positive and negative filling factor range marked by the grey-dashed frames in panel (c).

magnetic fields and high quality samples for which the width of the zeroth LL has been observed to be nearly temperature-independent.[4] The latter behavior has been attributed to reduced scattering owing to the presence of pronounced electron and hole puddles. In case of such diminished impurity scattering, charge transport is governed by a temperature-independent intrinsic scattering length rather than the temperature-dependent localization length responsible for the scaling within the higher Landau levels.

In order to determine the temperature exponent κ, the width of the zeroth LL is plotted in Fig. 2(b) as a function of temperature for two different Corbino devices of size 1.0 before and after annealing. From the slope of the linear fits in the double-logarithmic plot, $\kappa = 0.16 \pm 0.05$ (the error margin relates to the variance between samples, for a given sample it is ± 0.01) is extracted. This value of κ was found for all investigated Corbino devices independent of annealing. It was furthermore observed that annealing does not alter κ, although it shifts the charge neutrality point towards smaller back gate voltages and slightly reduces the absolute width. The value of $\kappa \sim 0.2$ is considerably smaller than $\kappa = 0.42$ documented for most conventional semiconductor 2DEGs characterized in Corbino or graphene Hall bar configuration.[1] At first sight, such reduction is surprising, since deviations to higher values are more common, and have been attributed to increased sample disorder.[17] According to scaling theory, κ is related to the universal scaling constant γ via $\kappa = p/2\gamma$, where p is the inelastic scattering exponent.[18] On this basis, the diminished κ could be due to a decrease in p or an increase in γ (or both). The value of p is governed by the scattering mechanism, i.e., p = 1 for electron-electron

scattering, $p = 2$ for acoustic phonon or piezoelectric scattering, and $p = 4$ for optical phonon scattering.[19] Which mechanism is predominant depends not only on the sample but also on the temperature range, such that universal scaling behavior might be observable below a certain temperature (e.g., for GaAs below 1 K (Refs. 13 and 20)). The universal scaling constant has been numerically derived to be $\gamma = 2.35 \pm 0.03$ under the assumption of $T = 0$ K.[2,3] This value has been experimentally confirmed for various 2DEGs like in AlGaAs/GaAs heterojunctions.[21] However, it should be emphasized that γ could be theoretically derived only for filled LL without spin degeneracy. For several filled LL and additional degeneracy, the situation is more complicated and leads to pronounced variation in the predicted value. Another limitation is that the calculations often neglect Coulomb interactions, and even when they are taken into account, there are still restrictions such as the assumption of ideal contacts.[16]

Insight into the origin of the small κ can be gained by a LL tail analysis which independently yields the value of γ. To this end, we evaluate the temperature dependent width of the zeroth LL for $\sigma_{xx} < \sigma_{fwhm}$, where the charge carriers are localized (shaded regions) and conduction occurs by variable range hopping (see Fig. 2(c)). Here, the temperature dependent conductivity is given by

$$\sigma_{xx} = \sigma_0 \exp\left(-\sqrt{T_0/T}\right), \tag{3}$$

with a characteristic temperature T_0 that depends on the Coulomb energy according to

$$T_0(\nu) = \frac{Ce^2}{4\pi\varepsilon\varepsilon_0 k_B \xi(\nu)}. \tag{4}$$

In this equation, C is a dimensionless constant on the order of unity, k_B is the Boltzmann constant, $\varepsilon_0 = 8.85 \times 10^{-12}$ C $V^{-1}\cdot m^{-1}$ is the vacuum permittivity, $\varepsilon \approx 2.5$ is the dielectric constant for graphene on Si/SiO_2,[22] and $\xi(\nu)$ is the filling factor dependent localization length[1]

$$\xi(\nu) = \xi_0 |\nu - \nu_c|^{-\gamma}. \tag{5}$$

Equation (5) allows determining the value for γ in the sample under investigation. Based upon Eq. (3), the characteristic temperature T_0 for the lowest LL can be determined from the slope of the $\ln(\sigma_{xx})$ vs. $1/\sqrt{(T)}$ plot for every filling factor value in the aforementioned shaded regions. In Fig. 2(d), thus obtained values are displayed as $\ln(T_0)$ in dependence of $\ln[(\nu - \nu_c)/4]$, where the 4 accounts for the 4-fold degeneracy of the LL. By combining Eqs. (4) and (5), the slope in this double-logarithmic plot then yields a value of $\gamma = 7.7 \pm 0.2$ for the filling factor range above the LL center ν_c and $\gamma = 6.9 \pm 0.2$ below the LL center ν_c ($\nu_c = 0$ for 0th LL and $\nu_c = 4$ for the 1st LL). A similar analysis for the other samples and also for higher LLs provides roughly the same value $\gamma = 7.6$ with a variance between the samples of ± 0.9, independent of the size of the Corbino devices. While the γ value $\gamma = 7.6$ considerably exceeds the theoretically expected value of $\gamma = 2.35$, combining it with the low value for κ in the present samples results in the expected inelastic scattering exponent of $p = 2$, which is also consistent with previous studies on graphene Hall bar devices.[4]

The value of $p = 2$ gains further support from the temperature characteristic of the LLs in dependence of the size of the Corbino devices. In Fig. 3(a), the temperature dependent width of the zeroth LL is compared between two high quality devices (on the same wafer) of size 1.0 and 0.75. For better comparison, the data points belonging to the size 0.75 device are shifted to match those of the size 1.0 device in the high temperature region. The larger width for the size 1.0 device is most likely a consequence of the sizeable degeneracy lifting. In both devices, the LL width reaches a plateau below a critical temperature T_c, where the scattering length L_ϕ approaches the sample dimensions corresponding to the graphene channel width L_{sample}. The values of T_c are determined to be 6.0 ± 0.5 K for $L_{sample} = 1.0\,\mu$m and 8.0 ± 0.5 K for $L_{sample} = 0.75\,\mu$m. This hints toward $L_{sample} \propto T_c^{-p/2} = T_c^{-1}$ dependence, thus consolidating the value of $p = 2$ in the present Corbino devices. At the critical temperature T_c, the LL width corresponds to a localization length which is equal to the effective length of the sample. This is illustrated for a 0.75 size device in Fig. 3(b), which reveals that for the zeroth LL width of $\Delta\nu = 1.86 \pm 0.03$ ($T_c = 8$ K), the localization length ξ coincides well with the sample size of $L_{sample} = 750$ nm. Having established the scaling of the lowest LL, comparison is made in Fig. 3(c) with the behavior of the first (electron and hole) LL in two devices of different quality. It is apparent that the first LLs saturate at lower temperatures, indicating that they have a shorter scattering length and that the zeroth LL is protected against scattering. The latter conclusion is in agreement with experiments using graphene Hall bar devices.[4]

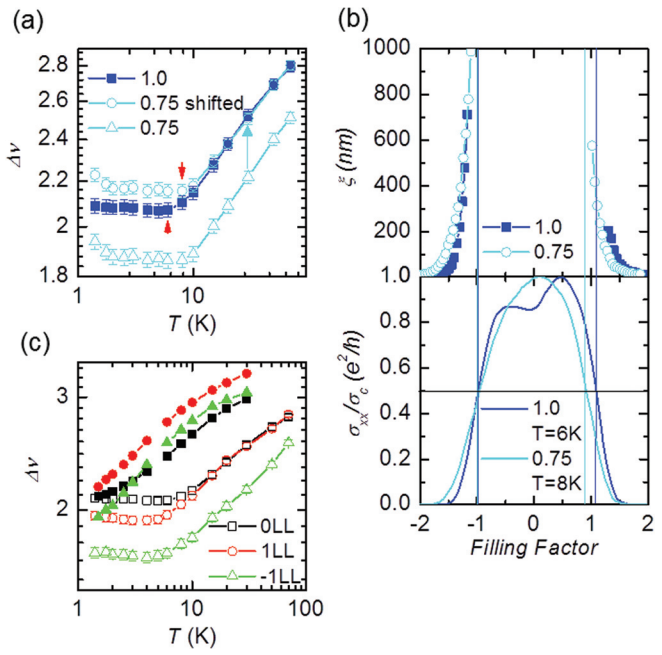

FIG. 3. (a) Temperature dependence of the FWHM of the zeroth LL in two Corbino devices of different size. Red arrows indicate the temperature at which the scattering length approaches the sample dimensions. (b) Localization length and width for the zeroth LL as a function of filling factor in a size 0.75 device. (c) Dependence of the width of the zeroth and first LL in one 1.0 device (filled symbols) and one 0.75 device (open symbols).

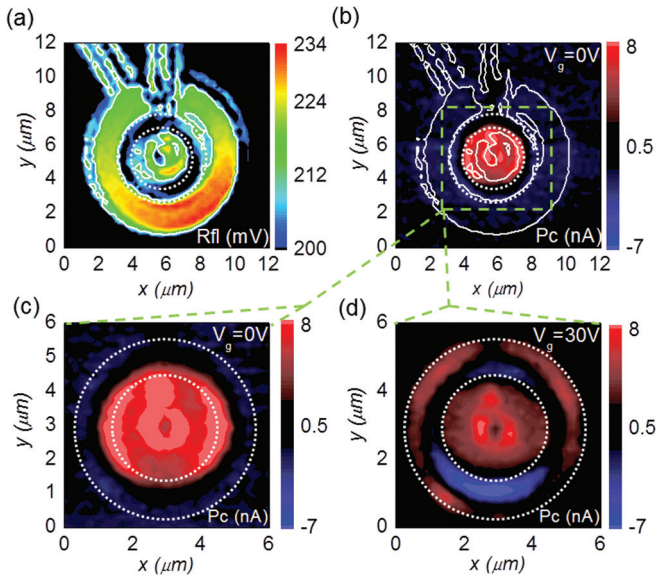

FIG. 4. (a) Optical reflection image of a size 1.0 Corbino device. (b) Zero-bias scanning photocurrent image of the device recorded at zero gate voltage (p-type regime). (c) Zoom into the photocurrent map in panel (b). (d) Zero-bias photocurrent map of the same device at a gate voltage of +30 V (n-type regime).

Valuable clues regarding the origin of the deviation of κ and γ could be gained from scanning photocurrent microscopy (SPCM) of the Corbino devices, as exemplified in Fig. 4. The SPCM image in Figure 4(b) exhibits pronounced photocurrent signals of opposite signs at the outer edge of the inner ring and the inner edge of the ring. These signals arise from charge separation by the potential steps formed at the metal contacts,[23] and hence provide a means to spatially map the potential distribution in devices. A zoom into photocurrent images acquired in the p- and n-type regime of the device (see Figs. 4(c) and 4(d), respectively) reveals that the signals are not equally distributed along the circular electrodes edges. Especially, the segregated and elongated lobes visible in the n-type regime indicate that doping due to the metal contacts alone cannot account for the observed photocurrent distribution. A reasonable explanation for the photocurrent pattern involves a macroscopic inhomogeneity of carrier concentration which could arise from the voltage applied to the bridge, or residues of the e-beam resist. Similar doping fluctuations have been documented to alter the scaling parameters in semiconductor 2DEGs,[17] albeit effects due to non-ideal contacts may also play a role.[16]

In summary, our magneto-conductance measurements demonstrate that an inhomogeneous charge carrier distribution in graphene Corbino devices can lead to the manifestation of an unusual scaling behavior, as reflected by a reduced temperature exponent of LL width and an increased universal scaling constant. However, this change does not affect the predominant scattering mechanisms in graphene that have been identified in previous graphene Hall bar studies.

[1]H. P. Wei, D. C. Tsui, M. A. Paalanen, and A. M. M. Pruisken, Phys. Rev. Lett. **61**, 1294 (1988).
[2]B. Huckestein and B. Kramer, Phys. Rev. Lett. **64**, 1437 (1990).
[3]B. Huckestein, Rev. Mod. Phys. **67**, 357 (1995).
[4]A. J. M. Giesbers, U. Zeitler, L. A. Ponomarenko, R. Yang, K. S. Novoselov, A. K. Geim, and J. C. Maan, Phys. Rev. B **80**, 241411(R) (2009).
[5]M. Amado, E. Diez, D. López-Romero, F. Rosella, J. M. Caridad, F. Dionigi, V. Bellani, and D. K. Maude, New J. Phys. **12**, 053004 (2010).
[6]M. Amado, E. Diez, F. Rosella, V. Bellani, D. López-Romero, and D. K. Maude, J. Phys.: Condens. Matter **24**, 305302 (2012).
[7]T. Shen, A. T. Neal, M. L. Bolen, J. J. Gu, L. W. Engel, M. A. Capano, and P. D. Ye, J. Appl. Phys. **111**, 013716 (2012).
[8]Y. Zhang, Z. Jiang, J. P. Small, M. S. Purewal, Y.-W. Tan, M. Fazlollahi, J. D. Chudow, J. A. Jaszczak, H. L. Stormer, and P. Kim, Phys. Rev. Lett. **96**, 136806 (2006).
[9]J. G. Checkelsky, L. Li, and N. P. Ong, Phys. Rev. Lett. **100**, 206801 (2008).
[10]A. J. M. Giesbers, L. A. Ponomarenko, K. S. Novoselov, A. K. Geim, M. I. Katsnelson, J. C. Maan, and U. Zeitler, Phys. Rev. B **80**, 201403 (2009).
[11]T. Kramer, C. Kreisbeck, V. Krueckl, E. J. Heller, R. E. Parrott, and C.-T. Liang, Phys. Rev. B **81**, 081410 (2010).
[12]P. A. Russell, F. F. Ouali, N. P. Hewett, and L. J. Challis, Surf. Sci. **229**, 54 (1990).
[13]T. Brandes, Phys. Rev. B **52**, 8391 (1995).
[14]S. Koch, R. J. Haug, K. v. Klitzing, and K. Ploog, Phys. Rev. Lett. **67**, 883 (1991).
[15]H. P. Wei, S. Y. Lin, D. C. Tsui, and A. M. M. Pruisken, Phys. Rev. B **45**, 3926 (1992).
[16]T. Ando, J. Phys. Soc. Jpn. **61**, 415 (1992).
[17]W. Li, J. S. Xia, C. Vicente, N. S. Sullivan, W. Pan, D. C. Tsui, L. N. Pfeiffer, and K. W. West, Phys. Rev. B **81**, 033305 (2010).
[18]D. J. Thouless, Phys. Rev. Lett. **39**, 1167 (1977).
[19]F. Hohls, PhD Thesis, University of Hannover (2000).
[20]T. Brandes, L. Schweitzer, and B. Kramer, Phys. Rev. Lett. **72**, 3582 (1994).
[21]S. Koch, R. J. Haug, K. von Klitzing, and K. Ploog, Surf. Sci. **263**, 108 (1992).
[22]O. Wunnike, Appl. Phys. Lett. **89**, 083102 (2006).
[23]E. J. H. Lee, K. Balasubramanian, R. T. Weitz, M. Burghard, and K. Kern, Nat. Nanotechnol. **3**, 486 (2008).